Talanta 222 (2021) 121480

Contents lists available at ScienceDirect

Talanta

journal homepage: www.elsevier.com/locate/talanta

Streaming-enhanced, chip-based biosensor with acoustically active, biomarker-functionalized micropillars: A case study of thrombin detection

Min Zhou [a], Dan Gao [a,*], Zhou Yang [b], Chao Zhou [b], Ying Tan [a], Wei Wang [b,**], Yuyang Jiang [a]

[a] State Key Laboratory of Chemical Oncogenomics, Tsinghua Shenzhen International Graduate School, Tsinghua University, Shenzhen, Guangdong, 518055, China
[b] School of Materials Science and Engineering, Harbin Institute of Technology (Shenzhen), Shenzhen, Guangdong, 518055, China

ARTICLE INFO

Keywords:
Microfluidic chip
Microstreaming
Thrombin
Immunoassay
Biosensor

ABSTRACT

Enzyme-linked immunosorbent assay is a widely used analytical technique for detecting and quantifying disease-specific protein biomarkers. Despite recent progresses in disease-specific protein biomarkers detection with microfluidic chips, many devices still suffer from the limited mass transport of target molecules, and consequently low detection efficiency or long incubation time. In this work, we present a novel strategy to significantly enhance the sensing efficiency of a chip-based biosensor by exploiting micro-streaming in an acoustofluidic device, which boosts intermolecular interactions and a hybridization chain reaction to increase the fluorescent signals. This device was made of a microfluidic chip that contains an array of PDMS micropillars in a ship-shaped microchannel. And the inner surface of the channel was functionalized with capture aptamers that bind with thrombin, chosen as a model target molecule. An ultrasonic transducer underneath the chip operating at 150 kHz generates circular micro-streaming flows around the pillars that significantly improves the binding efficiency of thrombin with capture aptamers by 1) increasing the retention time and 2) enhancing mass transport via local convection versus diffusion. The effects of ultrasound parameters, such as operating frequencies and voltages, on the distribution and magnitude of flows were optimized to obtain a better performance of the sensor chip. Under the optimized conditions, the detection limit was increased by one order of magnitude. Although this work has focused on the detection of thrombin as a model molecule, this streaming-enhanced, microstructure-based sensing strategy can be applied to detect a wide range of molecules or even cells.

1. Introduction

Enzyme linked immunosorbent assay (ELISA) is the most frequently used technique for protein analysis [1,2]. This technique has attracted mounting interest in current clinical diagnosis due to its high sensitivity and specificity. However, conventional ELISA is labor-intensive, time--consuming, and requires large amounts of antigens and sample volumes [3]. In addition, the mass transport of biomolecules in an immunoassay is pivotal for their binding kinetics and ultimately influences the sensor's performance [4]. However, most of the current sensing system mainly rely on Brownian diffusion, which puts a significant limit on the detection sensitivity and speed (hours to days) [5]. To improve the sensing performance, incubation for an extended period is commonly used to allow the reaction to proceed sufficiently. However, to achieve a higher reaction efficiency by prolonging reaction time is often non-ideal for practical applications [6,7].

The above-mentioned issues with ELISA can be improved to some degree by increasing the reaction surface area and enhancing mass transport by microfluidic techniques, which open up new opportunities for numerous biological, medical and pharmaceutical applications [8,9]. For example, a valid strategy was the introduction of micropillars into microchannels to increase the surface-to-volume ratio for the interaction between target and recognition molecules, resulting in a higher capture efficiency [10,11]. Thanks to the high surface-to-volume ratio at micro/nano scales of a miniaturized device, considerable time can be saved due to the reduced diffusion distances. Cost can also be significantly reduced due to a much smaller reagents consumption. However, even though the diffusion distance was significantly decreased in microfluidic channels, rapid mixing in the direction of flow remains difficult because of the nature of laminar flows at low Reynolds number [12], which becomes a hindrance to an efficient reaction.

Two strategies have been proposed to enhance mass transport in a

* Corresponding author.
** Corresponding author.
E-mail addresses: gao.dan@sz.tsinghua.edu.cn (D. Gao), weiwangsz@hit.edu.cn (W. Wang).

https://doi.org/10.1016/j.talanta.2020.121480
Received 22 March 2020; Received in revised form 10 June 2020; Accepted 27 July 2020
Available online 13 August 2020

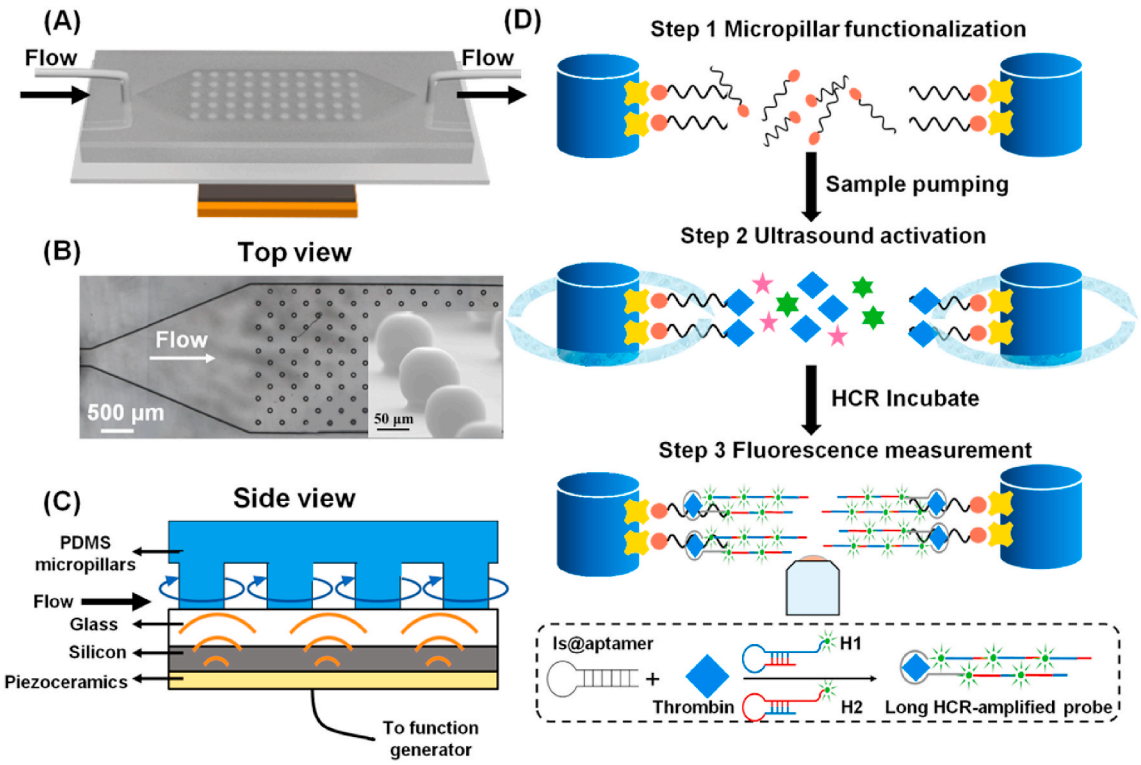

Fig. 1. Schematic illustration of the biosensor based on an acoustofluidic chip. (A) 3D rendering of the acoustofluidic chip. Structures are drawn for illustrative purpose and not to scale; (B) Top view of the microfluidic chip under an optical microscope. Inset: a SEM image of the micropillars; (C) A cartoon illustration of the side view of the chip. Circular streaming pattern is generated around each PDMS pillar, which is bond with the bottom glass substrate. A piezoelectric ceramic disk glued to the bottom of the chip generates ultrasound. (D) Schematic of the thrombin detection process.

microfluidic channel: passive or active mixing. Passive mixing in a microchannel is usually achieved by decreasing the diffusive mixing distance [13], or by generating chaotic advection, such as spiral circulations and 3D vortices, and microstructured channel walls [13]. Active mixing, on the other hand, can be realized by applying optical tweezers [14], platform design [15], magnetic stirring [16] or acoustic technique [17–21] to generate local flows that enhance mixing. Among the various active mixers used in microfluidic channels, acoustic mixers based on a micro-streaming effect has emerged as a powerful technique that is simple to implement and control. Acoustic streaming is a hydrodynamic effect, arising from the attenuation of the sound waves passing through a medium [22,23]. In particular, the energy dissipation of sound waves crossing a solid-liquid interface generates a local, steady micro-streaming flow that is commonly found in many acousto-fluidic devices containing bubbles [24], sharp edges [25], and beams of surface acoustic waves impinging on device walls [26]. Among the various structures, vibrating cylinders immersed in liquid have long been known to generate two pairs of streaming vortices [27,28]. Experiments done in the early 2000s reproduced similar patterns with microscopic cylinders [29,30], and interesting 2D arrays of vortices were observed later within micropillar arrays in a microfluidic channel [31–33]. Although the power of microstreaming has been exploited to mix chemicals [25,30], as well as to trap cells [26,34], microorganisms [33] and other microparticles [31,32], its usefulness in biosensing, and particularly in accelerating immunoassays, has remained limited [35–40].

2. Experimental section

2.1. Materials

SU-8 2050 negative photoresist were purchased from Microchem (Newton, CA). Polydimethylsiloxane (PDMS) were purchased from Dow Corning (Sylgard 184, Midland, MI). Streptavidin (1KU), 4-Maleimidobutyric acid N-hydroxysuccinimide ester (GMBS), 3-Mercaptopropyltrimethoxysilane (MPTS), thrombin (TB), transferrin (TRF), acyl carrier protein (ACP), human serum albumin (HSA) and bovine serum albumin (BSA) were purchased from Sigma Aldrich (U.S.A). Tween 20 was purchased from Sangon Biotechnology Co. Ltd. (Shanghai, China). All the oligonucleotides used in experiments were synthesized and purified by Sangon Biotechnology Co. Ltd. (Shanghai, China).

2.2. Chip design and modification

A ship-shape microchannel containing a PDMS micropillar array was designed for thrombin detection (See Fig. 1 for illustrations). In detail, the channel was 1.2 cm long, 2.5 mm wide and 100 μm deep. PDMS micropillars were designed within the channel. The microfluidic device was fabricated using standard soft lithography and replica molding techniques described elsewhere [41]. The detailed process of the device fabrication is shown in Supporting Information.

Before experiments, the microfluidic system was sterilized by exposure to UV light for 30 min and the microchannel was rinsed with 75% ethanol. The microchannel was then modified with specific aptamers for thrombin capture. Surface modification and capture aptamer fixation were performed according to the methods described in the literature [15,42]. The device was then treated with freshly prepared 0.01 μmol/mL GMBS ethanol solution for 30 min at room temperature. Next, the channel was filled with 10 μg/mL streptavidin in PBS for 1 h. Finally, a biotin-labeled thrombin capture aptamer solution with a concentration of 20 μg/mL was introduced and incubated at room temperature for 30 min, followed by washing with PBS to remove unbonded capture aptamers. The device was stored at 4 °C for further use.

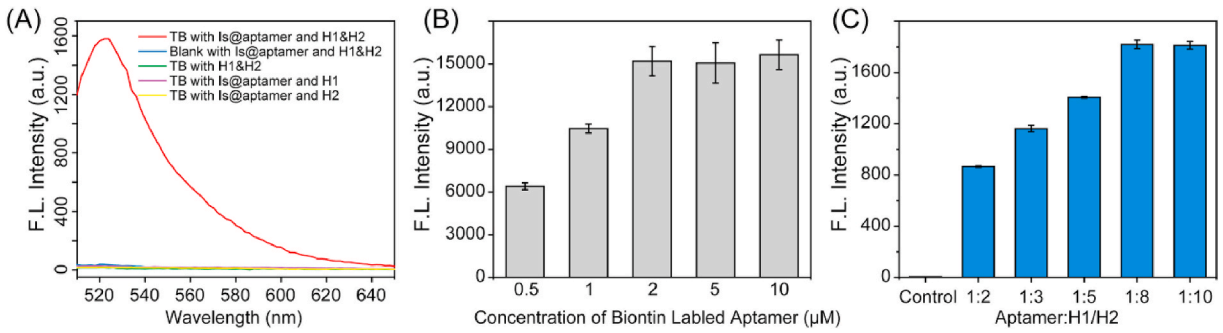

Fig. 2. The working principle evaluation of the proposed assay and optimization curve of experimental reagent dosage. (A) Experimental proof of the proposed immunoassay and (B) optimization of Is@aptamer concentration and (C) ratio of Is@aptamer and H1/H2. The standard error bars means the variation of three independent experiments.

2.3. Detection of thrombin on the microfluidic chip using HCR signal amplification strategy

HCR was employed as a signal amplification strategy for the detection of thrombin on the microfluidic chip. It was a series of cascade hybridization reactions initiated by the initiation chain in an enzyme-free environment at room temperature, which was first put forward by Dirks and Pierce [43]. The sequences used in the HCR system were the same as the work reported by Ma et al. [44] They were listed as below (from 5′ to 3′, it is noted that sticky ends are underlined and the initiating sequence of aptamer (Is@aptamer) is bold).

H1. AGTAGGTTGTATAGTTCAAAGTAACTATACAACCTACTACCTCA-FAM

H2. FAM-ACTTTGAACTATACAACCTACTTGAGGTAGTAGGTTGTATAGTT

Is@aptamer: **TGAGGTAGTAGGTTGTATAGTT**AGTCCGTGGTAGGGCAGGTTGGGGTGACT

Before injecting HCR related reagents into the microfluidic channels, they were pretreated by the following two steps. Firstly, FAM-labeled hairpin DNA probes (H1 and H2) and Is@aptamer sequences were heat-annealed in separate tubes at 95 °C for 2 min. They were then gradiently cooled with 1 °C per mintue to room temperature for 1 h before use. Different samples were then introduced into the microfluidic channels modified with the thrombin captured aptamers, and the device was incubated at room temperature for 45 min with or without the drive of acoustic streaming for thrombin capture. PBS solution was then injected into the channels to wash the unbounded molecules. Finally, the mixture of 500 nM Is@aptamer and 4 μM H1/H2 in PBS buffer (0.1 M, pH 7.4) were injected into the channels and incubated for 1 h at room temperature for HCR signal amplification, and the fluorescence intensity of the reaction system was detected using the inverted fluorescence microscope.

2.4. Ultrasonic streaming enhanced thrombin detection on chip

Acoustic streaming was used to enhance the local fluid flow in the microchannel by a low-frequency acoustic filed. To be specific, a piezoelectric ceramic transducer (Steminc inc. SMD12T06R412WL, nominal resonance frequency 3.4 MHz) was glued by epoxy to the back of the microfluidic device, with the center of the ceramic disk underneath the channel. The two electrodes of the transducer were connected to a wavefunction generator that outputs sinusoidal signals (Keysight, 33510B). A voltage amplifier (Falco, WMA-300, 50X amplification) was used to generate a final voltage of 25–125 $V_{p\text{-}p}$. In our experiments, a frequency range from 120 to 160 kHz was tested, outside of which streaming became negligible. Note that this frequency range is much lower than the resonance frequency of the transducer, and therefore limits the outputted ultrasound power. Polystyrene (PS) microspheres (2 μm in diameter) were added to the channel as flow tracers, and their speeds were used to represent the fluid flow within a microfluidic channel, particularly near the micropillars. In a typical experiment, the sample solution was first injected into the microfluidic channel, followed by turning on the ultrasound so that micro-vortices were generated around micropillars. Thrombin solutions were then injected into the channel. Experiments with different streaming periods were performed by varying the duration of optimized ultrasound power (0, 10, 20, 30 and 40 min, respectively) for the reaction between thrombin and aptamer, followed by elution with PBS. Then the HCR signal amplification mixtures prepared in the previous steps were injected into the channel and was allowed to react at room temperature for 1 h. Finally, the fluorescence signal was collected by an inverted fluorescence microscope (Leica, DMB4000B) with a mercury lamp as the excitation source.

3. Results and discussion

3.1. Schematic illustration of acoustofluidic biosensor device

A schematic of the acoustofluidic biosensor device used in the current experiment is shown in Fig. 1A. The ship-shaped channel was designed to facilitate the solution injection and decrease the dead-volume inside the channel. In order to increase the surface-to-volume ratio of the channel to improve the thrombin capture efficiency, we designed an array of PDMS micropillars. According to the experimental results, an arrangement of micropillars that was too dense lead to chaotic flow and easy formation of air bubbles. The optimized arrangement consisted of a PDMS layer containing an array of micropillars (diameter 100 μm with 400 μm spacing) in a rectangular area (5 mm × 2.5 mm) bond to a glass slide substrate (Fig. 1B). Mass transport of biomolecules in an immunoassay is crucial for their binding kinetics and ultimately influences the sensor's performance. The enhanced mass transport was mainly achieved by generating microstreaming in the channel around the micropillars after turning on ultrasound (Fig. 1C). In addition, in order to achieve specific capture of thrombin, the PDMS micropillars were modified with aptamers. Stable fluorescence signal was finally obtained by enhancement from streaming and HCR signal amplification (Fig. 1D).

3.2. Working principle of immunoassay in acoustofluidic device

In this work, a pair of hairpin DNA probes (H1 and H2), each with a fluorophore at the sticky end, was designed specifically for HCR signal amplification to detect thrombin, each with a fluorophore at the sticky end. A "sandwich" assay was adopted, where the target was captured by the capture aptamer immobilized on the surface of the channel and micropillars. An initiator strand that can specifically recognize thrombin was injected into the channel, the hairpin structure of H1 was opened,

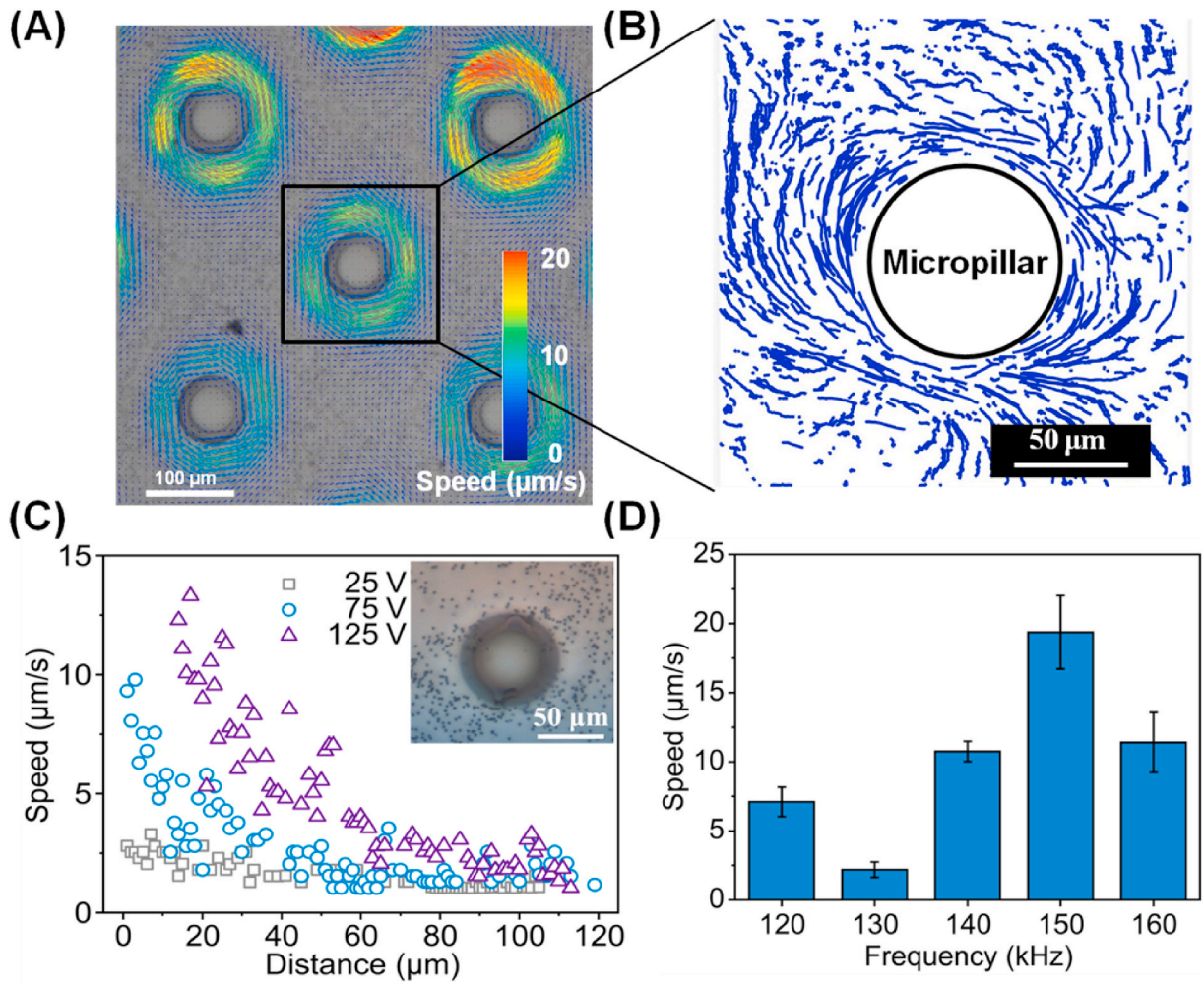

Fig. 3. Characterization of micro-streaming around micropillars. (A) Particle Image Velocimetry (PIV) result of the fluid around the PDMS micropillar; (B) Trajectories of tracers (2 μm PS) around a PDMS micropillar; (C) Speed of tracers at different distances from a micropillar under different ultrasound driving voltages. The ultrasound frequency was fixed at 150 kHz; (D) Speed of tracers around the micropillars when the ultrasound frequency was changed from 120 kHz to 160 kHz, with an ultrasound voltage fixed at 100 V.

releasing the hybridization energy. H1 and H2 polymerize non-covalently to form a long nicked double-helix analogue [43]. The used initiator strand has the initiating function at the 3′ end and recognition function at the 5' end. The fluorescence signal was expected to enlarge due to the amplified probes on the assembled double-helix analogue generated from the modified fluorophore of H1 and H2, resulting the sensitivity improvement.

To verify that the fluorescence was indeed generated from thrombin initiated HCR-amplified probe assembly, additional experiments were carried out using conventional method by microplate reader without the existence of some parameters of the HCR-amplified system. Before HCR-amplified system, H1, H2, and Is@aptamer were annealed separately and mixed together before assembly incubation. As the red curve shown in Fig. 2A, only when the target thrombin was present and with the coexist of H1, H2 and Is@aptamer, the opened aptamer-induced fluorescence was generated which was undoubtedly resulted from HCR.

The concentration of the biotin labeled capture aptamer that specific to thrombin was firstly investigated to ensure the completely modification of the inner surface of the channel by the aptamer. We used a biotin-labeled capture aptamer with a fluorescein (FAM) probe for direct detection by confocal fluorescence microscope. As shown in Fig. 2B, when the concentration of the biotin-labeled capture aptamer increased from 0.5 μM to 10 μM, the fluorescence signal remained nearly the same at the concentration of 2 μM which means the saturated modification at this concentration. Therefore, we used 2 μM biotin-labeled capture aptamer for inner surface modification in the following experiments.

To obtain the optimal performance of the fluorescence signal of HCR-amplified system, the molar ratio between the Is@aptamer and the two hairpin chains H1 and H2 was also evaluated on chip. Fig. 2C indicated that Is@aptamer with 8-fold H1/H2 can fully complete the assembly. The result was in accordance with the data reported in the previous literature [45]. As the incubation time was critical for on chip HCR, we prolonged the time from 0 to 40 min. As can be seen from Fig. S2 in Supporting Information, the fluorescence signal got saturated at the incubation time of 30 min.

During the binding of thrombin to the capture aptamer, the ultrasound was loaded into the channel of the microfluidic chip to generate microvortices in the channel, and the thrombin was rotated to increase the contact efficiency between the capture aptamer and thrombin.

3.3. Acoustic microstreaming near micropillars

As was introduced earlier, microstreaming often occurs near vibrating micropillars and the device was immersed in water to energy dissipation. Although two pairs of vortices are typically observed in systems vibrated along the x or y direction, recent experiments and simulations suggest that rotational vibration of micropillars produces circular microstreaming around pillars [34,46–48]. This was indeed

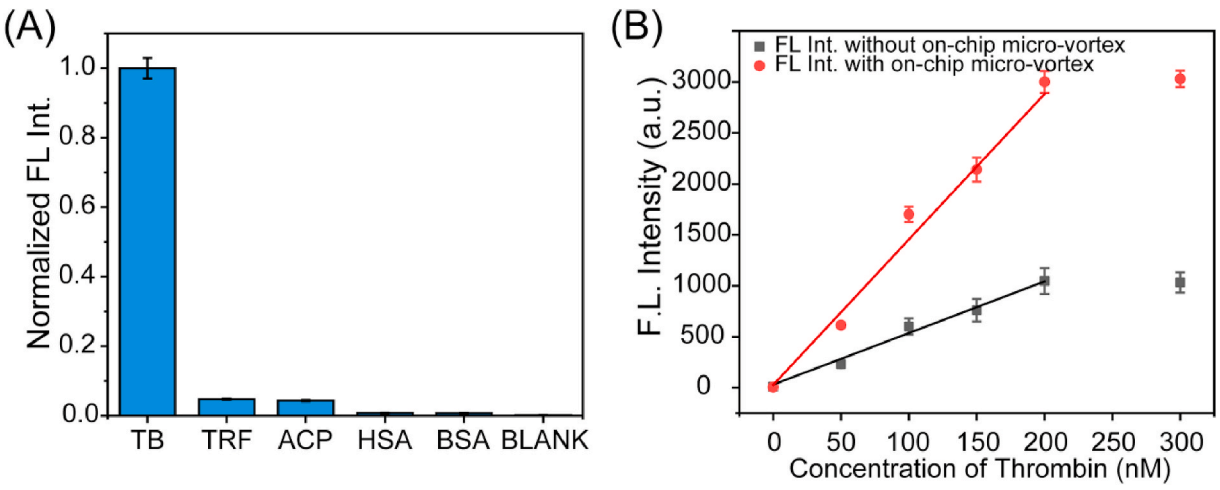

Fig. 4. Specificity evaluation of the detection platform and the relationship between fluorescence intensity and thrombin concentration. (A) Specificity evaluation of the detection platform. (B) Relationship between fluorescence intensity and thrombin concentration, each point was the average of three measurements. (insert is the linear curve for thrombin). The red curve is for the situations with on chip microvortex, whereas the black curve is for that without on chip microvortex. (For interpretation of the references to colour in this figure legend, the reader is referred to the Web version of this article.)

observed in our system, where circular flows emerged near micropillars located above the transducer upon turning on the ultrasound at ~150 kHz (Fig. 3A). We note the following two features of this microstreaming. First, the rotation direction (clockwise or counter-clockwise, Fig. 3B) around each micropillar was the same, but this directionality could vary upon changing the driving frequency. Second, the flow magnitude, as measured by tracking tracer particles, decays gradually away from the vicinity of the pillar to the bulk (see measurement in Fig. 3C). This flow profile was qualitatively the same as that acquired by a previous study of circularly vibrating micropillars [48].

Because the magnitude of the streaming, and thus the effectiveness of the enhancement of mass transport, is sensitive to changes in the ultrasound frequencies and voltages, we carried out experiments to quantify this correlation. First, the output voltage was increased from 25 V to 125 V, while the frequency was set to 150 kHz (Fig. 3C). Flow speeds at a radial distance of 10 μm–100 μm from the edge of the pillars were measured by tracking the speeds of tracer particles orbiting pillars. Results shown in Fig. 3C suggests that, intuitively, a high driving voltage produces stronger streaming flows, with a peak speed at a driving voltage of 125 V that was ~5 times faster than that at 25 V. Driving frequencies, on the other hand, affect the flow speeds in a less linear way. Different experiments conducted at frequencies ranging from 120 to 160 kHz (Fig. 3D) show that fastest streaming (~20 μm/s @ 100 V) occurred at 150 kHz, while frequencies below or above this optimal frequency resulted in less effective streaming. This frequency is likely the resonance frequency of the micropillars, but a detailed investigation of the vibration modes of these pillars is beyond the scope of this study.

Based on the above quantification, a driving voltage of 100 V and a frequency of 150 kHz were chosen as the optimal parameters to yield fast, yet regular flow patterns (higher voltages could lead to chaotic mixing and more severe heating). These parameters were used for all of the immunoassay experiments reported in this study. We note that heating at such a high driving voltage is inevitable, and this issue is mitigated in our experiments by installing a homemade water-cooling stage on the microfluidic device. Realistically, the heating issue can be largely resolved by choosing a piezoelectric transducer with a resonance frequency close to the operating frequency (i.e. 150 kHz), which will in principle eliminate the use of a power amplifier.

3.4. Specificity and sensitivity of the immunoassay for thrombin on the microfluidic device

The specificity of the biosensor depends on the affinity of the aptamer, and several common proteins in human serum were detected to evaluate the specificity of the platform. The experiments were performed on chip without acoustic field. All the proteins were at the concentration of 100 nM. These proteins were added to the detection system separately. After the incubation was completed, the reaction solution was rinsed out, and the amplification related reagents were injected into the chip. As shown in Fig. 4A, only the target thrombin had a considerable fluorescence intensity. The common proteins, including transferrin (TRF), acyl carrier protein (ACP), human serum albumin (HSA), and bovine serum albumin (BSA), had only low and negligible fluorescence intensity. The results indicated that the assay had the analytical ability to detect thrombin in a complex biological environment.

In order to make better use of this assay, a serial concentrations of thrombin were detected on chip under optimal conditions with and without acoustic field to obtain the working curves referring to corresponding fluorescence intensity. The calibration curves are shown in Fig. 4B. A linear relationship between thrombin concentration and relative fluorescence intensity was observed with the concentration ranged from 0.1 to 200 nM. The fluorescence intensity of thrombin gradually increased with increasing thrombin concentration. Without the acoustic field, the equation for the calibration curve is $I_1 = 8.64393 + 5.06796 \times C_{Thrombin}$, $R_1^2 = 0.9905$. As for the assays under the acoustic field, the calibration curve is $I_2 = 5.31856 + 14.2814 \times C_{Thrombin}$, $R_2^2 = 0.9863$. The detection limit was calculated by 3σ rule (see Supporting Information) [49]. The results showed that after the application of acoustic field, the detection limit increased about 10 times from 139 pM to 15 pM because of the passive mixing produced by the acoustic rotary microsystem. The results demonstrated that the efficiency of thrombin detection can be significantly improved by loading a fluid-enhanced acoustic module on a microfluidic chip. Our developed method can also be extended to other molecules or cells detections.

3.5. Human serum sample assay

In order to evaluate the analytical reliability and application potential of our established platform, human serum samples obtained from Shenzhen People's Hospital were processed for thrombin detection. The patients or their legal representative gave written informed consent for all investigations and inquires that were conducted in this study. Human studies were approved by the Medical Ethics Committee of the hospital. To overcome the interference of background fluorescence, serum samples were firstly diluted to different times with PBS buffer (0.1 M, pH

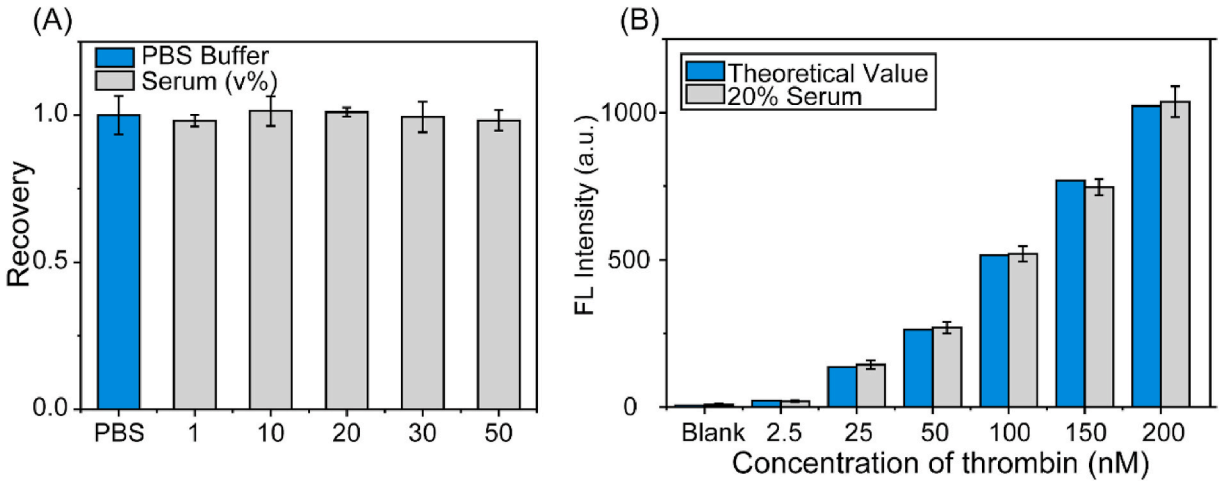

Fig. 5. Results of human serum sample assay. (A) The fluorescence intensity with 50 nM thrombin spiked in buffer, 1%, 10%, 20% 30% or 50% human serum; (B) The fluorescence intensity of different concentrations of thrombin in 20% human serum, compared with theoretical values based on theoretical curves. The standard error bars mean the variation of three independent experiments.

7.4). Different amounts of human serum samples were then spiked with 50 nM thrombin for its detection using our developed method. As shown in Fig. 5A, when the content of serum increased from 1% to 50%, the fluorescence signals were almost the same as the original signal in the buffer. The results indicated that our biosensor had an excellent anti-interference ability which is suitable for the application in complex biological samples. Furthermore, several serum samples were prepared by incorporating different amounts of thrombin into a 20% serum sample to obtain the final concentration ranged from 2.5 nM to 200 nM. And 20% serum sample without additional added thrombin was used as a blank to investigate whether the proteins in the serum have interference on the final fluorescence signal. The corresponding fluorescence intensities of the thrombin at these concentrations were calculated according to the working curve. As displayed in Fig. 5B, the theoretical value was nearly the same to that in 20% serum sample. And the 20% serum sample has nearly no fluorescence signal. Moreover, the recovery rate in human serum was between 94.13% and 106.06%. Acoustic streaming in a microfluidic device provides a new insight into thrombin-related assay. These results indicate that the sensor platform developed has great potential for thrombin detection in real biological samples, which was critical to disease diagnosis. Besides, in order to improve the detection sensitivity, other sensitive measuring strategies like chemiluminescence can be exploited in the future.

4. Conclusion

In conclusion, we demonstrated an acoustofluidic chip biosensor with a micropillar array that generates acoustic microstreaming. Accelerated mass transport by acoustic streaming significantly enhances the binding efficiency between the nucleic acid capture aptamer and the target molecule thrombin, thereby improving the detection sensitivity by at least one order of magnitude. The current device design can be improved in the following two aspects to further enhance its mixing capability. First, the streaming flows generated by the current chip are slower than typical streaming speeds reported in the literature by roughly one order of magnitude [47]. Possible limitations include the weak bonding between the PDMS pillars and the glass substrate, strong acoustic damping by PDMS pillars are soft, and the use of a piezoelectric ceramic transducer with an inappropriate resonance frequency. Silicon pillars fabricated by etching a Si wafer can solve the first two problems, and replacing the transducer will improve the third issue. Second, as illustrated by the large-scale flow mapping in Fig. 3A and Fig. S3 in Supporting Information, much of the areas in the channel remain un-touched by streaming. This was partly due to the same inefficient flow mentioned above, and partly because of the geometric designs of our micropillar arrays that inevitably left un-reachable pockets of fluids. Molecules within those "dead" pockets have to rely on diffusion to reach a vortex, from which point the mass transport begins to accelerate. A better design of pillar array can in principle mitigate this issue, while balancing the presence of chaotic flows we discovered with arrays of a higher density. Although this article has focused on the detection of thrombin as a model molecule, this streaming-enhanced, microstructure-based sensing strategy can be applied to the capture and detection of a wide range of molecules or even cells.

Credit author statement

Min Zhou: Data curation, Investigation, Writing-Original draft preparation. Dan Gao: Conceptualization, Methodology, Writing-Reviewing and Editing. Zhou Yang: Data curation, Investigation, Writing-Original draft preparation. Chao Zhou: Data curation, Investigation, Writing-Original draft preparation. Ying Tan: Supervision. Wei Wang: Conceptualization, Methodology, Writing-Reviewing and Editing. Yuyang Jiang: Supervision

Declaration of competing interest

The authors declare that they have no known competing financial interests or personal relationships that could have appeared to influence the work reported in this paper.

Acknowledgements

This work was supported by the National Natural Science Foundation of China (No. 21675096, 11774075), Natural Science Foundation of Guangdong Province, China (No. 2020A1515010660) and Key-Area Research and Development Program of Guangdong Province, China (No. 2019B020209009).

Appendix A. Supplementary data

Supplementary data to this article can be found online at https://doi.org/10.1016/j.talanta.2020.121480.

References

[1] X. Yu, Y. Xia, Y. Tang, A nanostructured microfluidic immunoassay platform for highly sensitive infectious pathogen detection, Small 13 (24) (2017).

[2] N. Chang, J. Zhai, B. Liu, Low cost 3D microfluidic chips for multiplex protein detection based on photonic crystal beads, Lab Chip 18 (23) (2018) 3638–3644.
[3] M.H.R. Kym, N. Baker, Ashvin Patel, M.H. Paul Boyd, Rapid monitoring of recombinant protein products a comparison of current technologies, Trends Biotechnol. 20 (4) (2002) 149–156.
[4] J.R. Gong, Label-free attomolar detection of proteins using integrated nanoelectronic and electrokinetic devices, Small 6 (8) (2010) 967–973.
[5] T.M. Squires, R.J. Messinger, S.R. Manalis, Making it stick: convection, reaction and diffusion in surface-based biosensors, Nat. Biotechnol. 26 (4) (2008) 417–426.
[6] D. Liu, X. Li, J. Zhou, A fully integrated distance readout ELISA-Chip for point-of-care testing with sample-in-answer-out capability, Biosens. Bioelectron. 96 (2017) 332–338.
[7] S.K. Arya, P. Estrela, Electrochemical ELISA-based platform for bladder cancer protein biomarker detection in urine, Biosens. Bioelectron. 117 (2018) 620–627.
[8] M. Devillers, L. Ahmad, H. Korri-Youssoufi, Carbohydrate-based electrochemical biosensor for detection of a cancer biomarker in human plasma, Biosens. Bioelectron. 96 (2017) 178–185.
[9] T. Yuan, D. Gao, S. Li, Coculture of tumor spheroids and monocytes in a collagen matrixembedded microfluidic device to study the migration of breast cancer cells, Chin. Chem. Lett. 30 (2) (2019) 81–86.
[10] P. Bandaru, D. Chu, W. Sun, A. Khademhosseini, A microfabricated sandwiching assay for nanoliter and high-throughput biomarker screening, Small 15 (15) (2019), e1900300.
[11] W. Sheng, T. Chen, R. Kamath, Aptamer-enabled efficient isolation of cancer cells from whole blood using a microfluidic device, Anal. Chem. 84 (9) (2012) 4199–4206.
[12] A.D. Stroock, S.K.W. Dertinger, A. Armand, Chaotic mixer for microchannels, Science 295 (5555) (2002) 647–651.
[13] C.-H. Lin, C.-H. Tsai, L.-M. Fu, A rapid three-dimensional vortex micromixer utilizing self-rotation effects under low Reynolds number conditions, J. Micromech. Microeng. 15 (5) (2005) 935–943.
[14] F. Mej, T.A. Nieminen, N.R. Heckenberg, Optical alignment and spinning of laser-trapped microscopic particles, Nature 394 (6702) (2003) 348–350.
[15] S.L. Stott, C.H. Hsu, D.I. Tsukrov, Isolation of circulating tumor cells using a microvortex-generating herringbone-chip, Proc. Natl. Acad. Sci. U. S. A 107 (43) (2010) 18392–18397.
[16] I. De Vlaminck, C. Dekker, Recent advances in magnetic tweezers, Annu. Rev. Biophys. 41 (2012) 453–472.
[17] D. Ahmed, A. Ozcelik, N. Bojanala, Rotational manipulation of single cells and organisms using acoustic waves, Nat. Commun. 7 (2016) 11085.
[18] T. Frommelt, M. Kostur, M. Wenzel-Schäfer, Microfluidic mixing via acoustically driven chaotic advection, Phys. Rev. Lett. 100 (3) (2008), 034502.
[19] T.-D. Luong, V.-N. Phan, N.-T. Nguyen, High-throughput micromixers based on acoustic streaming induced by surface acoustic wave, Microfluid. Nanofluidics 10 (3) (2011) 619–625.
[20] C. Suri, K. Takenaka, H. Yanagida, Chaotic mixing generated by acoustic streaming, Ultrasonics 40 (1–8) (2002) 393–396.
[21] K. Sritharan, C. Strobl, M. Schneider, Acoustic mixing at low Reynold's numbers, Appl. Phys. Lett. 88 (5) (2006), 054102.
[22] M. Wiklund, R. Green, M. Ohlin, Acoustofluidics 14: applications of acoustic streaming in microfluidic devices, Lab Chip 12 (14) (2012) 2438–2451.
[23] N. Riley, Steady streaming, Annu. Rev. Fluid Mech. 33 (1) (2001) 43–65.
[24] D. Ahmed, X. Mao, J. Shi, A millisecond micromixer via single-bubble-based acoustic streaming, Lab Chip 9 (18) (2009) 2738–2741.
[25] P.H. Huang, Y. Xie, D. Ahmed, An acoustofluidic micromixer based on oscillating sidewall sharp-edges, Lab Chip 13 (19) (2013) 3847–3852.
[26] D.J. Collins, B.L. Khoo, Z. Ma, Selective particle and cell capture in a continuous flow using micro-vortex acoustic streaming, Lab Chip 17 (10) (2017) 1769–1777.
[27] M.F. Hamilton, Y.A. Ilinskii, E.A. Zabolotskaya, Acoustic streaming generated by standing waves in two-dimensional channels of arbitrary width, J. Acoust. Soc. Am. 113 (1) (2003) 153–160.
[28] J. Holtsmark, Boundary layer flow near a cylindrical obstacle in an oscillating, incompressible fluid, J. Acoust. Soc. Am. 26 (1) (1954) 26.
[29] B.R. Lutz, J. Chen, D.T. Schwartz, Microfluidics without microfabrication, Proc. Natl. Acad. Sci. U. S. A 100 (8) (2003) 4395–4398.
[30] B.R. Lutz, J. Chen, D.T. Schwartz, Characterizing homogeneous chemistry using well-mixed microeddies, Anal. Chem. 78 (5) (2006) 1606–1612.
[31] T.A. House, V.H. Lieu, D.T. Schwartz, A model for inertial particle trapping locations in hydrodynamic tweezers arrays, J. Micromech. Microeng. 24 (4) (2014), 045019.
[32] V.H. Lieu, T.A. House, D.T. Schwartz, Hydrodynamic tweezers: impact of design geometry on flow and microparticle trapping, Anal. Chem. 84 (4) (2012) 1963–1968.
[33] T. Hayakawa, Y. Akita, F. Arai, Parallel trapping of single motile cells using vibratin-induced flow on microfluidic chip, in: 2017 IEEE 30th International Conference on Micro Electro Mechanical Systems (MEMS), 2017, https://doi.org/10.1109/MEMSYS.2017.7863652.
[34] X. Lu, A. Martin, F. Soto, Parallel label-free isolation of cancer cells using arrays of acoustic microstreaming traps, Adv. Mater. Technol. (2018) 1800374.
[35] R.H. Liu, R. Lenigk, R.L. Druyor-Sanchez, Hybridization enhancement using cavitation microstreaming, Anal. Chem. 75 (8) (2003) 1911–1917.
[36] D.K. Boraker, S.J. Bugbee, B.A. Reed, Acoustic probe-based ELISA, J. Immunol. Methods 155 (1) (1992) 91–94.
[37] E. Galopin, M. Beaugeois, B. Pinchemel, SPR biosensing coupled to a digital microfluidic microstreaming system, Biosens. Bioelectron. 23 (5) (2007) 746–750.
[38] Y. Bourquin, J. Reboud, R. Wilson, Integrated immunoassay using tuneable surface acoustic waves and lensfree detection, Lab Chip 11 (16) (2011) 2725–2730.
[39] A. Renaudin, V. Chabot, E. Grondin, Accelerated surface plasmon resonance biosensing by surface acoustic waves microstreaming, in: 2011 6th IEEE International Conference on Nano/Micro Engineered and Molecular Systems, IEEE, 2011, pp. 1140–1143.
[40] L.A. Kuznetsova, W.T. Coakley, Applications of ultrasound streaming and radiation force in biosensors, Biosens. Bioelectron. 22 (8) (2007) 1567–1577.
[41] Y. Chen, D. Gao, H. Liu, Drug cytotoxicity and signaling pathway analysis with three-dimensional tumor spheroids in a microwell-based microfluidic chip for drug screening, Anal. Chim. Acta 898 (2015) 85–92.
[42] M.G. Ahmed, M.F. Abate, Y. Song, Isolation, detection, and antigen-based profiling of circulating tumor cells using a size-dictated immunocapture chip, Angew. Chem. Int. Ed. 56 (36) (2017) 10681–10685.
[43] R.M. Dirks, N.A. Pierce, Triggered amplification by hybridization chain reaction, Proc. Natl. Acad. Sci. U. S. A 101 (43) (2004) 15275–15278.
[44] D. Sturtevant, Y.J. Lee, K.D. Chapman, Matrix assisted laser desorption/ionization-mass spectrometry imaging (MALDI-MSI) for direct visualization of plant metabolites in situ, Curr. Opin. Biotechnol. 37 (2016) 53–60.
[45] J. Chen, Z. Huang, Z. Luo, Multichannel-structured three-dimensional chip for highly sensitive pathogenic bacteria detection based on fast DNA-programmed signal polymerization, Anal. Chem. 90 (20) (2018) 12019–12026.
[46] X. Lu, K. Zhao, H. Peng, Local enhanced microstreaming for controllable high-speed acoustic rotary microsystems, Phys. Rev. Appl. 11 (4) (2019).
[47] X. Lu, F. Soto, J. Li, Topographical manipulation of microparticles and cells with acoustic microstreaming, ACS Appl. Mater. Interfaces 9 (44) (2017) 38870–38876.
[48] K. Kaneko, T. Osawa, Y. Kametani, Numerical and experimental analyses of three-dimensional unsteady flow around a micro-pillar subjected to rotational vibration, Micromachines 9 (12) (2018).
[49] Y. Zhang, J. Xia, F. Zhang, A dual-channel homogeneous aptasensor combining colorimetric with electrochemical strategy for thrombin, Biosens. Bioelectron. 120 (2018) 15–21.